F.R. Note No. 141/1955

20 FEB 1956

DEPARTMENT OF SCIENTIFIC AND INDUSTRIAL RESEARCH AND FIRE OFFICES' COMMITTEE
JOINT FIRE RESEARCH ORGANIZATION

THE DISTRIBUTION OF TEMPERATURE AND VELOCITY DUE TO FIRES BENEATH CEILINGS

by

F. H. Thomas

Summary

The distributions of gas temperature and velocity due to a fire beneath flat and open-joisted ceilings have been measured and are discussed on the basis of elementary theory. Scaling is briefly discussed and data are given for two fires of different size. Some experimental and calculated values for the operating times of a fire alarm are discussed.

November, 1955.

Fire Research Station,
Boreham Wood,
Herts.

THE DISTRIBUTION OF TEMPERATURE AND VELOCITY DUE TO FIRES BENEATH CEILINGS

by

P. H. Thomas

1. Introduction

As part of the study of the behaviour of sprinklers and fire alarms, some experiments have been made of the effect of the ceilings on the distribution of temperature and velocity of heated gases from a fire. This knowledge is of importance in the siting of heat sensitive fire detectors beneath open-joisted and flat ceilings.

Fire detectors at the ceiling receive heat from a developing fire by radiation and convection. In the transfer of heat to the ceiling as a whole or to any large body near the source of heat radiation is of primary importance, whereas in the transfer of heat to a small body such as a thermocouple or the heat-sensitive element of a fire alarm, convection may be of comparable if not of greater importance.

2. Small-scale fires - Experimental

Small-scale experiments were made with a 17 in. diameter circular tray of burning methylated spirit. This was supported $4\frac{1}{2}$ ft. below a flat ceiling and temperature measurements were made at various distances up to 8 ft. from the fire and at various distances up to 12 in. beneath the ceiling. The thermocouples used were of chromel-alumel wire 0·0048 in. diameter. The radiation correction was negligibly small except over the fire where the measured gas temperature was about 20°C too high.

Some experiments were also made under an open-joisted ceiling, the joists being [illegible] in. x 1 in. and spaced 16 in. apart.

Velocity measurements with a 4 in. diameter vane anemometer could only be made where the heated gases were fairly cool (c.50°C) and this meant that data were obtained only at 8 ft. from the centre of the ceiling. In future work more detailed velocity measurements will be necessary.

2.1. Small-scale fires - Results for flat ceiling

The rate of burning of the tray fire is shown in Figure 1, and the distribution of temperature along the ceiling and perpendicular to it are shown in Figures 2 and 3, it is seen that the temperature falls almost inversely with the distance along the ceiling for distances greater than about 2 ft. The mean velocity over the 4 in. below the ceiling was 2·6 ft/sec and between 4 in. and 8 in. below the ceiling about 1·3 ft/sec.

2.2. Discussion

2.2.1. The conservation of momentum

The pressure gradient in the heated layer below the ceiling will be dependent on the changing thickness of the layer and the temperature gradient along the ceiling.

Thus if is the mean temperature in a layer of thickness Δ

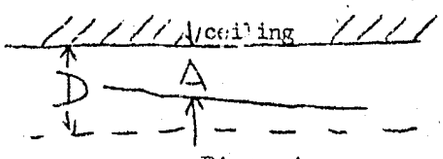

Figure 4

the pressure at the ceiling is less than at a distance D below the ceiling by an amount approximately

$$P = \rho_0 g (D - \Delta) + \rho_\theta g \Delta \qquad (1)$$

where ρ_0 and ρ_θ are the densities corresponding to the ambient temperature and the temperature θ respectively. The ratio of the mean radial pressure gradient to the momentum gradient is

$$R = \frac{\frac{1}{2}\rho \frac{dp}{dr}}{\bar{u} \frac{d\bar{u}}{dr}} \qquad (2)$$

where $\bar{u}$ is the root mean square velocity of the heated gas stream and r is the radial distance.

If we assume the thickness Δ to be constant over a short region we have from equations (1) and (2)

$$R \doteq \frac{g \frac{\Delta}{T_0} \frac{d\theta}{dr}}{2\bar{u} \frac{d\bar{u}}{dr}} \qquad (3)$$

where T_0 is the absolute ambient temperature.

In these experiments we assume

$$\bar{\theta} \propto \frac{1}{r^n}$$

and (see 1.1a)

$$\bar{u} \propto \frac{1}{r^n}$$

Hence equation (3) becomes

$$R \doteq \frac{g \Delta \bar{\theta}}{2 T_0 \bar{u}^2} \qquad (4)$$

In the experiments Δ may be taken to be approximately 4 in. and if the velocity 8 ft. from the centre of the ceiling is 1.5 ft/sec and the mean temperature 25°C we have, from equation (4)

$$R_8 = 0.20$$

At about 2 ft. from the centre of the ceiling for 100°C and say 6 ft/sec

$$R_2' = 0.05$$

Since R_2' is small it follows that the variation of pressure may be regarded as having negligible effect on the conservation of momentum near the ceiling centre but the effect becomes larger as the distance from the centre increases, and the conservation of momentum can only be used as a first approximation in calculation when r becomes large.

2.2.2. Estimation of velocity of gas stream

Neglecting the effect of pressure in the heated layer and the friction of the ceiling we have for the conservation of momentum

$$r \int_0^\infty \rho u^2 dy = \text{constant} \qquad (5)$$

where u is velocity at a distance "y" below the ceiling. Neglecting the heat transferred to the ceiling the conservation of heat gives

$$r\int_0^{\infty} \rho u \theta \, dy = \text{constant} \qquad (6)$$

where θ is the temperature above ambient of the gases at a distance "y" below the ceiling. Until the ceiling temperature has risen appreciably the boundary conditions for velocity and temperature rise are the same, i.e. both are zero at and far from the ceiling. Thus comparing equations (5) and (6) we have

$$u(r) \propto \theta(r) \qquad (7)$$

where and are maxima or mean values perpendicular to the surface. Theoretical treatments (‡) of the problem are not entirely satisfactory and usually refer to distances large compared with the size of the source. Prandtl's momentum-transfer theory suggests that for similar boundary conditions the velocity and temperature distribution should be equal whereas Taylor's velocity-transfer theory suggests that the temperature distribution is the square root of the velocity distribution for equal boundary conditions. Further theoretical considerations are given below.

A linear velocity gradient is assumed which will fit the experimental data at 8 ft. this is

$$u = 3{\cdot}3\ (1 - 1{\cdot}2\ y)\ \text{ft/sec} \qquad (8)$$

where "y" is measured in feet.
Equation (7) now enables us to estimate the velocity of the gases at any r. At the centre of the ceiling the maximum velocity is approximately given by $3{\cdot}3 \times \frac{200}{47}$ i.e. 14 ft/sec. This may be compared with an estimated value from the buoyancy effect of the flames.

The pressure difference between the base of the flames provides the gains in velocity head of the cold air entering the flame and the acceleration of gases on heating in the flame. If all the entrainment of air is assumed to occur at the base of the flame and the cross section of the flames is assumed constant we can calculate the velocity in the region at 200°C just above the flames as follows. See Fig (5) -

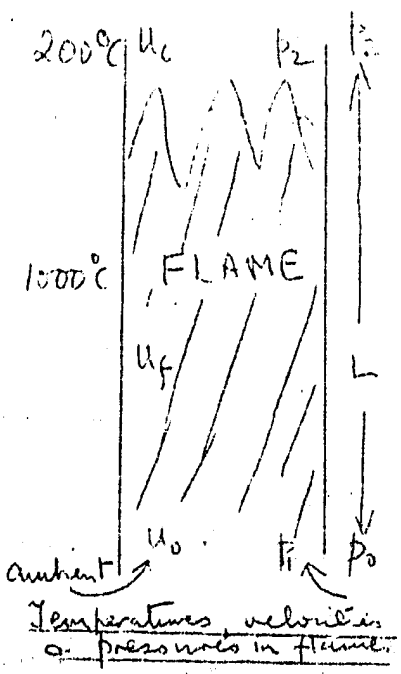

Fig. 5

We have the continuity relations

$$u_0 \rho_0 = u_f \rho_f = u_1 \rho_1 = m \qquad (9)$$

and the density equations

$$\frac{\rho_0}{T_0} = \frac{\rho_f}{T_f} = \frac{\rho_c}{T_c} \qquad (10)$$

T denoting absolute temperature.
The equations of flow are

$$p_0 - p_1 = \frac{\rho_0 u_0^2}{2g} \qquad (11)$$

$$p_1 - p_2 = m(u_c - u_0) + \rho_f L \qquad (12)$$

and $$\rho_0 L = p_0 - p_2 \qquad (13)$$

Adding these equations (11), (12) & (13) and making use of (9) and (10) we have

$$u_c = \frac{T_c}{T_0}\sqrt{\frac{2gL\left(\frac{T_f - T_0}{T_f}\right)}{1 + 2\left(\frac{T_c - T_0}{T_0}\right)}}$$

‡ Some problems of two dimensional turbular jets are discussed by Goldstein.(1) See also Batchelor (2) and Koestel (3) for recent reviews.

Inserting $T_o = 300°K$ $T_c = 500°K$ $T_r = 1300°K$ and $L = 3$ ft.

We have

$$U_c = 13.3 \text{ ft/sec.}$$

This is a maximum estimate which allows for no drag due to the entraining of air outside the flame and compares favourably with the other estimate. The closeness of the agreement is probably fortuitous as both estimates are probably too high.

2.2.3. The conservation of heat

The heat transferred to the ceiling may be estimated approximately as follows.

The local heat transfer coefficient for a turbulent boundary layer, at a distance x along a flat plate is given by (4)

$$N_{Nu} = 0.029 \; N_{Pr}^{\frac{1}{3}} \; N_{Re}^{0.8}$$

where N_{Nu} is the Nusselt No. $\frac{hx}{K}$

N_{Pr} is the Prandtl No. ν/k

N_{Re} is the Reynold's No. $\frac{ux}{\nu}$

and h is the heat transfer coefficient
K is the thermal conductivity of the gases
ν is the kinematic viscosity of the gases
k is the thermal diffusivity of the gases
and u is the velocity of the gases

For these gases the Prandtl No. may be taken as 0.71 and then the Nusselt No. N_{Nu} is related to the Reynolds No. N_{Re} by the following expression

$$N_{Nu} = 0.026 \; N_{Re}^{0.8} \qquad (14)$$

Beyond a radius of 2 ft. we may take velocity and temperature as inversely proportional to r. Fig. (2 and 3). We therefore take

$$\theta = \frac{370}{r} \qquad (15)$$

and from equations (7) and (8)

$$u = \frac{26}{r} \qquad (16)$$

where r is in ft.

Since data for radial flow heat transfer are not available we assume equation (14) for a flat plate to apply to this case.

we have $\nu = 26 \times 10^{-5} \text{ ft}^2/\text{s}$ at 100°C
$K = 8 \times 10^{-5}$ C.G.S. units at 100°C

and the total heat transfer within the annulus $8' > r > 2'$ is calculated as 2,000 cals/sec. Within a circle of radius 2 ft. u is taken as 13 ft/sec and θ as 200 and the heat transfer is calculated as 870 cals/sec i.e. a total of nearly 3,000 cals/sec.

The total heat in the gases at radius $8'$.

is $$Q = 2\pi . 8 . C \rho \int_0^\infty u . \theta . dy$$

Where ρ, C are the density and specific heat at constant pressure of the gases at 25°C. The experimental data for temperature and the assumed distribution for velocity (equation (8)) at a radius of 8 ft. were integrated and the value for Q calculated as 16,800 cals/sec. The heat lost to

the ceiling is thus about $\frac{3000}{20,000} = 15\%$. The rate of burning of the fire having a diameter of 17 cms. was 0·52 lb/min which was equivalent to a rate of heat production of 24,000 cals/sec assuming complete combustion. If the flames are assumed to be 17 in. diameter and 3 ft. high with an emissivity of 0·2 the total radiation for a temperature of 1000°C is about 5,000 cals/sec i.e. a net rate of heat passing into the gas stream and the ceiling by convection of about 19,000 cals/sec as compared with nearly 20,000 cals/sec estimated directly.

The agreement of this figure with the sum of the heat transferred to the ceiling and in the gas stream 8 ft. from the centre of ceiling is better than might be expected in view of the approximations made.

3. The effects of scale - Flat ceilings

3.1. Large-scale experiments

Some experiments reported elsewhere (5) have been made to compare the behaviour of two types of sprinkler under various conditions and as a secondary consideration some data on ceiling temperatures and their spatial distribution were obtained. The ceiling was 20 ft. square supported at a height of 10 ft. by brick pillars at the four corners. The burning material was straw in a fibreboard lattice similar to an egg-box, each compartment being of side 3 ft. 3 in. and containing $6\frac{1}{2}$ lb of straw.

The fire was ignited in a box beneath the centre of the ceiling and allowed to spread. In fact the straw in this box was largely consumed by the time the fire had spread to the adjoining boxes, this led to a fall in temperature after the initial rise. Eight tests of this type under a flat ceiling were made and were essentially similar as far as the development of the fire was concerned. The distance of the fire from the ceiling was thus 10 ft. and the area of the one compartment in which the fire was contained for the initial period of growth 10·5 sq.ft. The small-scale fire of 1·57 sq.ft. was $4\frac{1}{2}$' from the ceiling. The results of these tests have been analysed and the mean temperature distribution for various times during the growth of the fire in the central compartment has been obtained. Since the temperature at the centre of the ceiling varied with time the temperatures at various distances from the centre are shown in Figure (6) as fractions of the central temperature. The data involves temperatures at the centre in the range 50° - 250° and it is seen that the ratio of temperatures elsewhere to that at the centre is largely independent of the maximum temperature in this range.

3.2. Discussion of fires of different size

We denote quantities referring to the smaller and larger fires by the suffixes 1 and 2 respectively. Neglecting the loss of heat to the ceiling we have

$$\Delta \nu \theta u \propto Q \tag{17}$$

where Q is the heat flow.
We have also

$$Q = \doteqdot R d^2 \tag{18}$$

where R is the rate of production of heat per unit area of fire and d is the diameter of the fire.
For any one fuel

$$R_1 = R_2$$

if the fires are large enough.

but if different fuels are used as in the two experiments reported here some relation must be adopted between R_1 and R_2. For this we assume the heat falling on the fuel from the flames is the same in both fires so that the rate of heat production is

$$R \propto C/I \tag{19}$$

where C is the calorific value per unit mass

and I is the total heat required to produce unit mass of combustible vapour. The flames from the spirit used in the tray tests were more similar in appearance to those from petrol rather than from alcohol and the assumption is made that they give of the same heat flux onto the fire surface. We now introduce the effective diameter D of the rising column of gases if the velocity were uniform over this diameter

Hence,
$$Q = \frac{\pi}{4} D^2 u_c \theta_c \rho c \tag{20}$$

where ρ and c are density and specific heat of rising gases, and the suffix 'c' refers to the centre of the ceiling.
It is expected that if the two fires are similar,

$$\theta/\theta_c = f(r/D)$$

Also from equation (7) we have

$$u/u_c = f(r/D)$$

Hence equation (17) becomes

$$Q \propto f^2 \Delta r \theta_c u_c \tag{21}$$

Therefore from equations (20) and (21)

$$\Delta r f^2 \propto D^2 \tag{22}$$

Therefore at equal values of r/D in the two experiments

$$\Delta \propto D \tag{23}$$

But from equations (18) and (20)

$$R d^2 \propto D u_c \theta_c \tag{24}$$

For equal central temperatures we have

$$u_c \propto \sqrt{L} \tag{25}$$

where "L" is the distance from the base of the fire to the ceiling.

Hence from equation (19), (24) and (25)

$$D \propto \frac{d}{L^{1/4}} \sqrt{\frac{C}{I}} \tag{26}$$

For the small-scale test we have for the spirit used

C = 7093 cals/gm (gross).
I = 255 cals/gm

For the larger fire, the fuel was straw and this is assumed to have a similar calorific value to wood. Assuming the surface temperature of the fuel to be 1,000°C and of the specific heat 0·3, we have

C = 3800 cals/gm (gross).
I = 300 cals/gm approximately.

The ratio of "L" for the two experiments was 2·12
so that

$$\frac{D_2}{D_1} = \frac{1}{1\cdot 8}\,\frac{d_2}{d_1}$$

Hence if θ/θ_c for the small-scale test is plotted against r/d_1 and θ/θ_c for the large-scale test against $1\cdot 8\, r/d_2$ there should be a single correlation. This is seen from Fig. (7) to be approximately so for small values of r, but the temperatures in the small-scale experiment are relatively higher further from the centre. We consider the flow through an elementary annulus as in Figure (8).

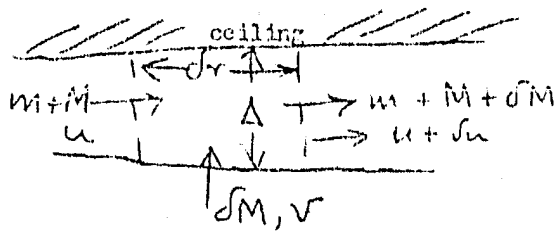

Fig. (8)

The entrained air enters the annulus with a velocity 'v' so that

$$\delta M = 2\pi r \rho v\, dr \qquad (27)$$

we also have

$$M+m = 2\pi r \rho \Delta \bar{u} \qquad (28)$$

and

$$\bar{\theta}(M+m) = m\,\theta_c \qquad (29)$$

where M is mass entrained in horizontal flow and 'm' is the mass arriving at the ceiling from below.

Hence from (29)

$$\frac{\theta}{\theta_c} = \frac{1}{\frac{M}{m}+1} \qquad (30)$$

and from (27) and (28)

$$\frac{dM}{M+m} = \frac{v}{\bar{u}}\,\frac{dr}{\Delta}$$

We assume for the present that the ratio of $\frac{v}{\bar{u}} = n$ is independent of either velocity or scale. This assumption is an alternative to the use of a momentum equation. The momentum has been shown to be only approximately constant

i.e.

$$\frac{dM}{M+m} = \frac{n\,dr}{\Delta} \qquad (31)$$

From Fig (3) it is seen that in the small-scale test Δ was largely independent of "r" in the range of "r" examined.

Hence from equations (30 and (31)

$$\theta/\theta_c = e^{-nr/\Delta} \qquad (32)$$

It is seen from Figure (7) where θ/θ_c is plotted against r/d that for the larger fire n/Δ is constant but is not so far the smaller fire. It is not possible to evaluate "n" without knowing Δ and this is only known in the range of r/d where the two curves diverge. In this range, the thickness of the layer in the small scale test is approximately 4 in. and if this value is taken, n equals 0·08. The ratio of v to the the maximum velocity u_m is approximately 0·04.

3.3. The thickness of the heated layer

It has been shown above that the thickness of the heated layer may be expected to be of the form

$$\Delta \propto \frac{d}{L^{1/4}} R \qquad (33)$$

where R is the rate of heat evolution per unit area of fire
d is the diameter of the fire.
and L is the distance of the fire below the ceiling.
In the small-scale experiment the thickness Δ was practically constant over a range in " " of 3 to 1. In the spreading of turbulent streams it is generally assumed that beyond a certain distance from the finite origin of the jet the spread may be taken as proportional to the distance along the axis of the stream. However the distances involved in these experiments are not large enough in relation to the size of the fire for this to be a reasonable assumption. Owing, moreover, to the buoyancy of the heated gases there is a pressure gradient along the stream which increases the momentum radially. Some attempt has been made to use von Kármán's momentum equation for the heated layer moving radially with a pressure term derived from the considerations given section (2·21), but further work must be done before a satisfactory analysis is possible.

4. Open joisted ceilings

4.1. Results for small scale fires

The temperature distribution under an open joisted ceiling is shown in Fig. (9). Along the centre gulley the temperature may be regarded as almost constant. The temperature along the ceiling across the joists is shown in Fig. (10) from which it is seen that it falls almost twice as rapidly as for a flat ceiling. The temperatures perpendicular to the ceiling for two positions along the axis perpendicular the direction of the joists are shown in Fig. (11).

The values of velocity 8 ft along the gulleys are shown in Table (1).

TABLE 1

Velocities in the gulleys of open joisted ceilings

	Velocity in ft/sec		
	Gulley over fire	Gullies next to one over fire	Gullies next but one to that over the fire
Top half of gulley	3·0	1·2	---
Lower half of gulley	2·5	1·3	1·2

4.2. Results for large-scale test

Figures 12 and 13 show the temperature distribution across the gulleys and along the centre gulley for a large scale fire similar to that described in section 3.1. At times less than 40 seconds there is negligible gradient along the gulleys but a large gradient across them. After 40 seconds the temperature gradient along gulleys seems to vary somewhat yet the temperatures 8 ft. from the centre and at the centre are a little different and both higher than at the intermediate distance. This anomaly is probably due to the results for the 2 2/3 ft. distance being averages of the two readings one on either side of the centre of the fire. Since the fire leaned slightly to one side the average values at 2 2/3 is too low. It is seen from Figure (12) that when the fire has developed so that the whole of the centre box is fully involved the gradient across the gulleys is less steep than it is when the fire is small and is approximately equal to that for a flat ceiling. This is to be expected since the larger the fire the smaller, relatively, are the joists. The opening times of sprinklers subjected to this developing fire were about 140 seconds for the open joisted ceiling compared with 100 - 110 seconds for a flat ceiling, and were in fact less than for sprinklers placed in the upright position under a flat ceiling. That the effect of the ceiling is less than the orientation of the sprinkler is confirmatory of the relatively small effect of the joists near a large fire.

The importance to be attached to the nature of the ceiling clearly depends on the size of the fire that can be tolerated before the operation of an alarm.

5. The siting of alarms and sprinklers

In view of the above discussion it follows that if a fire is to be detected in its early stages it would be preferable to adopt a distribution such as is shown in Figure (14) to the one shown in Figure (15).

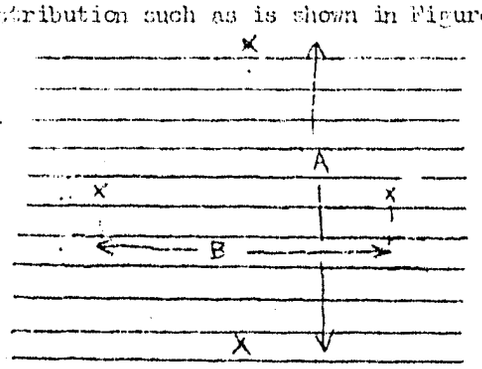

Figure (14)

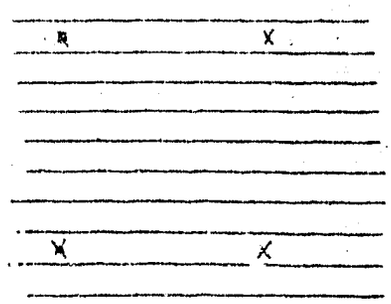

Figure (15)

In Figure (14) the greatest number of gullies to be crossed by the gas stream before arriving at a gulley containing an alarm is two instead of the three in Figure (15) and it would even be advantageous to decrease 'A' at the expence of 'B'. With flat ceilings there is a boundary layer close to the ceiling and alarms should be as near the ceiling as possible without being obscured in any way from the fire and without being in the boundary layer. This boundary layer increases with distances from the fire and is greater the slower the initial velocity of the gases. For longitudinal turbulent flow over a flat plate the boundary layer thickness is given by[4]

$$\delta = 0.38 \cdot x \left(\frac{u x}{\nu}\right)^{-0.2} \qquad (34)$$

where "x" is the distance from the plate edge. We take the velocity as 10 ft/sec., the kinematic viscosity for air at 100°C as 26×10^{-5} ft^2/sec and "x" as 5 ft.

Hence from equation (34)

$$d = 0.19 \text{ ft.} = 2 \text{ to } 3 \text{ in.}$$

This may be taken as the minimum distance that alarms or sprinklers should be placed below the ceiling. The greatest distance that should be permitted depends primarily on the size of fire to be tolerated. Since the thickness of the heated layer in the large fire test is, for a temperature just below the ceiling of 200°C, theoretically approximately 1.5 times that occuring with the smaller tray fire, the spacing from the ceiling should be kept as small as possible (less than 6 in. say) if reliance is put on the convection from heated gases. A large fire will produce greater radiation than does a small fire and a greater distance can be permitted if the size of the tolerated fire is relatively large. For spacings of about 12 in., the operation will be almost entirely by radiation.

6. Opening times of alarms and sprinklers

This is discussed in terms of a particular experiment. The discussion, however, is quite general. The fire was as in the 17 in. diameter tray tests under a flat ceiling. The sensitive element of the alarm was a bimetallic strip parallel to the ceiling. Two positions of the alarm were tested, one, the element projecting below the flat ceiling and two, the element in the plane of the ceiling, the body of the alarm was recessed.

Let h be the coefficient of heat transfer by convention between the heated gas stream and the exposed surface of the sensitive element.

Let H be the heat transfer by radiation per unit area of the exposed surface of the sensitive element.

Let A be the heated area of the sensitive element.

Let C be the thermal capacity of the heated part of the sensitive element.

We assume that the heating is slow enough in relation to the thickness of the sensitive element for this to be heated uniformly throughout its thickness.

Let θ_g be the temperature above ambient of the heated gases.

Let θ_e be the temperature above ambient of the element.

The heat balance equation for the heated element is thus

$$H + h(\theta_g - \theta_e) = \frac{C}{A}\frac{d\theta_e}{dt} \qquad (35)$$

If θ_g is assumed constant equation (35) can be integrated to give

$$\theta_e = (\theta_g + H/h)\left(1 - e^{-\frac{Ah}{C}t}\right)$$

If θ_p is the operating temperature of the alarm and t_p is the time of operation

$$t_p = -\frac{C}{Ah}\ln\left(1 - \frac{\theta_p}{\theta_g + H/h}\right) \qquad (36)$$

6.1. The evaluation of h - projecting alarm

For a flat plate exposed to the gas stream by being placed away from the ceiling so that it is out of the ceiling boundary layer we have for small plate and a lamina boundary layer (4)

$$N_{Nu} = 0{\cdot}66\ N_{Re}^{\frac{1}{2}} \qquad (37)$$

where the characteristic dimension "L" is the length of the plate.

For velocities of up to 10 ft/sec the Reynold's number for a $2\frac{3}{4}$ in. long plate is about 10^4 so that the boundary on the plate is laminar. Hence the use of equation (37) is justified. The heat transfer coefficient is then given by

$$h = \frac{0{\cdot}66K\ U_m^{\frac{1}{2}}}{L^{\frac{1}{2}}\ \nu^{\frac{1}{2}}} \qquad (38)$$

Taking ν as 19×10^{-5} ft^2/sec L as $2\frac{3}{4}$ in. and K as 7×10^{-5} C.G.S. units we have

$$h_1 = 0{\cdot}23 \times 10^{-3}\ U_m^{\frac{1}{2}} \quad \text{cals cm}^{-2}\ \text{sec}^{-1}\ {}^{\circ}\text{C}^{-1} \qquad (39)$$

where U_m is measured in ft/sec.

6.2. Evaluation of h - alarm flush with ceiling

If the plate is parallel to the ceiling we require the local heat transfer coefficient at the point on the ceiling a distance " r " from the centre. There does not appear to be any data for radial flow past a plate so we take as an approximation the formula for longitudinal flow. i.e. we use equation (14) where the characteristic dimension is the distance from the centre of the ceiling. Hence if U_m is in units of ft/sec and "r" is in ft. we have

$$h = \frac{0{\cdot}058 \times 10^{-3}}{r^{0{\cdot}2}}\ U_m^{0{\cdot}8} \quad \text{cals cm}^{-2}\ \text{sec}^{-1}\ {}^{\circ}\text{C}^{-1} \qquad (40)$$

6.3. The evaluation of H

If T_F is the absolute flame temperature assumed 1,000 C
ϵ is the emissivity of the flames.
ϕ is the configuration factor at the element.
and σ Stephan's constant

$$H \doteqdot \sigma \phi \epsilon T_F^4 \quad \text{approximately} \qquad (41)$$

is taken as 0·2. Since this may be as much as twice too great, the determination of H is very approximate, but since radiation is less important than convection in this experiment it does not affect the results greatly.

To determine ϕ we consider the flames to be equivalent to a rectangular area 4 ft. 6 in. high x 17 in. wide perpendicular to ceiling as in Figure (16).

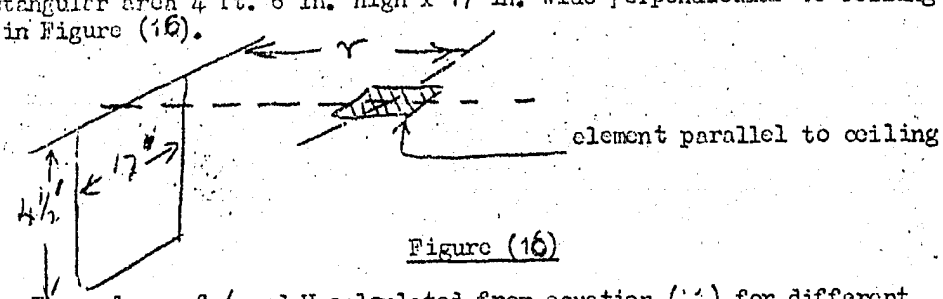

Figure (16)

The values of ϕ and H calculated from equation (41) for different values of "r" are given in Table (2).

TABLE (2)

Calculated configuration factors and radiation

"r" (ft)	ϕ	H cals cm^{-2} sec^{-1}
$3\frac{1}{3}$	0·027	0·019
$4\frac{1}{3}$	0·020	0·014
$6\frac{1}{3}$	0·010	0·007
$7\frac{1}{3}$	0·008	0·0056

Values of H for a flame temperature of 1,000°C can now be calculated and are also given in Table (2).

Data for the velocities at various points had to be assumed. It has been shown elsewhere that maximum velocities U_m for various points along the ceiling for this fire may be estimated from equation (7), (15) and (16):-

i.e. $$U_m = \frac{Q_s}{14}$$

where U_m is in ft/sec.

In addition we have

A = 13·3 sq. cm for a heated length of 7 cm
and C = 0·77 cal/°C.
The total thermal capacity for a length of 8·5 was found experimentally as 0·95 cal/°C. Before applying these data to calculate " " from equation (36) we must investigate the effect of uneven heating on the operation of the bimetallic strip. The alarms used had a rated operating temperature of 65°C. If it is assumed that this refers to uniform heating and that the ambient temperature is 17°C it can be shown that heating through a boundary layer of a thickness which increases from the fixed end of the strip to the free end, it can be shown that a mean rise in strip temperature of less than 48°C will operate the alarm. This is discussed in Appendix I where it is shown that for the condition of these experiments a mean temperature ranging from 38°C to 42°C according to the time of operation are sufficient.

This, although applying to the projecting alarm assuming convection to be predominant to radiation does not apply to the alarm in the plane of the ceiling where the boundary layer may not be expected to vary much over the length of the heated strip. Thus taking the values given in Appendix I as the effective operating temperature for the projecting alarm and 50°C for the alarm in the plane of the ceiling, we may calculate from equation (36) the opening times for the two alarms. These and the measured times are given in Table (3).

TABLE (3)

Opening times for alarm above tray fire

Distance from centre of fire (ft)	Operating times (sec)			
	Bimetallic strip 2 in. below ceiling		Bimetallic strip in plane of ceiling	
	Measured	Calculated	Measured	Calculated
$3\frac{1}{3}$	30	34	52	79
$4\frac{1}{3}$	33	54	53	122
$6\frac{1}{3}$	90	112	250	262
$7\frac{1}{3}$	144	161	Did not open in 300 secs	370

The results for the test at [illegible] ft. suggest the alarms may not have been adequately cooled after the previous test. Otherwise the agreement is as satisfactory as can be expected in view of the nature of the assumptions made.

7. Discussion and Conclusions

Some experimental data for the velocity and temperature distribution have been partly interpreted in the light of heat transfer theory, and there is some evidence that experiments may be scaled in size, though this would require more experimental data than is available at present for the principle to be made use of.

Elementary theory would seem to be insufficient to account for the apparent constancy of the thickness of the heated layer. Also it is necessary to measure the velocity of the heated gases directly at various points of the flow pattern in any future work. The heat transferred to the ceiling is, for the fires of the size discussed here, a small fraction, about 15 per cent of the total heat available, so that the use of a formula valid for longitudinal flow for flow from a central axis may well be sufficiently accurate. However, if it is desired to estimate this quantity closely this method of calculation is open to objection. Measurements rather than estimates made of flame radiation for different fires would be required as well.

The results that have been obtained show that some further consideration must be given to the siting of alarms and sprinklers. For flat ceilings it has been shown that the sensitive element must be at least 2 in. below a flat ceiling and any gas flow to it unobstructed. If the alarms are, say, 12 in. below the ceiling they will operate only if the radiation is great enough for the fire directly beneath them. A comparison of flat and open joisted ceilings shows that the latter may make a considerable difference in the early stages of a fire. This suggests that the square lattice arrangement is, from the aspect of detection, less sensitive than the diamond lattice.

APPENDIX I

The bimetallic strip operates by deflecting its free end a certain amount.

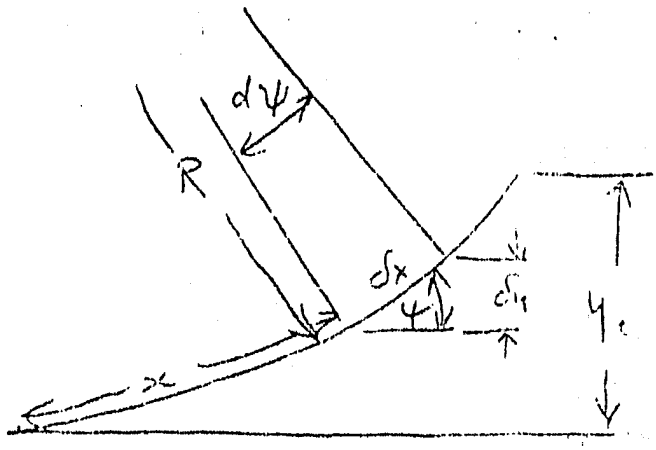

Figure (17)

Deflection of bimetallic strip

From Figure (17) we have

$$\frac{dy}{dx} = \sin\psi \doteq \psi \tag{42}$$

and

$$\frac{d\psi}{dx} = \frac{1}{R} \tag{43}$$

We assume that the curvature at any "x" is proportional to the local rise in temperature.

i.e.

$$\frac{1}{R} = B\theta \tag{44}$$

Hence from equations (42), (43), and (44)

$$\frac{d^2y}{dx^2} = B\theta$$

and

$$y_e = B\int_0^{\ell} dx \int_0^{x} \theta\, dx \tag{45}$$

For uniform heating we have

$$y_e = \frac{B\,\ell^2\theta}{2} \tag{46}$$

The alarm operates when y_e reaches a critical value y_c

i.e.

$$y_c = \frac{B\ell^2\theta_p}{2} \tag{47}$$

Hence from equations (45 and (47)

$$\theta_p = \frac{2}{\ell^2}\int_0^{\ell} dx \int_0^{x} \theta\, dx \tag{48}$$

where θ_c is the distribution of uneven heating producing operation of the alarm.
We now define a critical strip mean temperature θ'_p

$$\theta'_p = \frac{1}{\ell}\int_0^{\ell} \theta_c \, dx \tag{49}$$

and we calculate the ratio

$$\frac{\theta'_p}{\theta_p} = \frac{\ell}{2}\,\frac{\int_0^{\ell}\theta\, dx}{\int_0^{\ell} dx \int_0^{\ell}\theta\, dx} \tag{50}$$

Neglecting conduction along the strip and assuming that the gas stream has a temperature greatly in excess of the temperatures reached by the strip we can write that the temperature at a point is proportional to $x^{-\frac{1}{2}}$. This, of course, will not hold good near x equal zero but if this form is inserted in equation (49) we obtain

$$\frac{\theta'_p}{\theta_p} = 0{\cdot}75$$

It is possible to take account of the effect of conduction along the strip even if it is not easy to allow directly for the lowering of heat transfer by the rise in temperature of the strip,.

We have approximately

$$-K\Delta\frac{d^2\theta}{dx^2} + \rho c\,\Delta\frac{d\theta}{dt} = \frac{A}{x^{1/2}} \tag{51}$$

where Δ is the strip thickness
K is the strip thermal conductivity
ρ is the strip density
C is the strip specific heat
A is a constnat.

We assume that no heat is lost at the ends of the ends of the strip i.e.

$$\frac{d\theta}{dx} = 0 \qquad \text{at } x = 0 \text{ and } \ell$$

We write $x = \frac{\ell z}{\pi}$ and take the cosine transform denoted by

$$\bar{\theta} = \int_0^{\pi} \theta \cos px \, dx$$

Hence

$$\frac{\pi^2 K\Delta p^2}{\ell^2}\bar{\theta} \;\; \rho c\,\Delta\frac{d\bar{\theta}}{dt} = \frac{A\sqrt{\pi}}{\ell}\int_0^{\pi}\frac{\cos px}{x^{1/2}}\,dx \tag{52}$$

For an initial temperature of zero we have from (52)

$$\bar{\theta} = \frac{A\ell^{3/2}}{\pi^{3/2}p^2 K\Delta}\left(1 - e^{-\pi^2 p^2 kt}\right)\int_0^{\pi}\frac{\cos p\alpha}{\alpha^{1/2}}\,d\alpha \tag{53}$$

where $k = K/\rho c$

Inverting the transform according to the form

$$\theta = \frac{\bar{\theta}_{p=0}}{\pi} + \frac{2}{\pi}\sum_{1,2,3.} \bar{\theta}\cos px$$

(54)

we have from equations (53) and (54)

$$\theta = \frac{2At}{\rho c \Delta l^{1/2}} + \frac{2Al^{3/2}}{\pi^{5/2} k \Delta} \sum_{1,23}^{\infty} \left[\int_0^{\pi} \frac{\cos p\alpha}{\alpha^{1/2}} d\alpha \right] \frac{\left(1 - e^{-\pi^2 p^2 kt}\right)}{p^2} \cos px$$

(55)

Also from equation (49)

$$\theta'_p = \frac{2At}{\rho c \Delta l^{1/2}}$$

Hence from equations (50) and (55)

$$\frac{\theta_p}{\theta'_p} = 1 + \frac{4}{\pi^{5/2}} \tau \sum_{1,35}^{\infty} \left(\int_0^{\pi p} \frac{\cos \alpha \, d\alpha}{\alpha^{1/2}} \right) \frac{\left(1 - e^{-p^2 \tau}\right)}{p^{9/2}} \quad (56)$$

where

$$\tau = \frac{\pi^2 kt}{l^2}$$

For zero conduction along the strip we have $\tau = 0$

i.e.

$$\frac{\theta_p}{\theta'_p} = 1 + \frac{4}{\pi^{5/2}} \sum_{1.35}^{\infty} \left(\int_0^{\pi p} \frac{\cos \alpha \, d\alpha}{\alpha^{1/2}} \right) \frac{1}{p^{5/2}}$$

An approximate evaluation of this gives the result 1·336 instead of 4/3. For k = 0·1 and l = 8·0 cm, we have $\tau = \frac{t}{65}$
Taking the observed values of "t" we calculate equivalent operating temperatures θ'_p from equation (56). Values are given in Table (4).

TABLE (4)

Equivalent operating temperatures

t	τ	θ_p/θ'_p	Equivalent operating temperature
30	0·46	1·257	38°C
33	0·51	1·227	39°C
90	1·38	1·166	41°C
144	2·22	1·123	42°C

Acknowledgments

The experimental observations with the tray fire were made by Mr. F. Hinkley and Mr. P. H. T. Smart; a vacation student, Mr. C. Knights, also assisted in the work.

References

(1) "Modern Developments in Fluid Dynamics". S. Goldstein. O.U.P. 1938.

(2) "Heat convection and buoyancy effects in fluids." G. K. Batchelor. Quat. J. R. Met. Soc. 1954, 80, 339-58.

(3) "Computing temperatures and velocities in vertical jets of hot or cold air", A. Koestel. Heating and Ventilating Research, 1, 1 Jan/march, 1955.

(4) "Introduction to the Transfer of Heat and Mass", Eckert McGraw hill 1950.

(5) "A comparison of the conventional and the "wide cover" type sprinkler," P. H. Thomas and F. Nash, Joint Fire Research Organisation F.R. Note No. 154/1955.

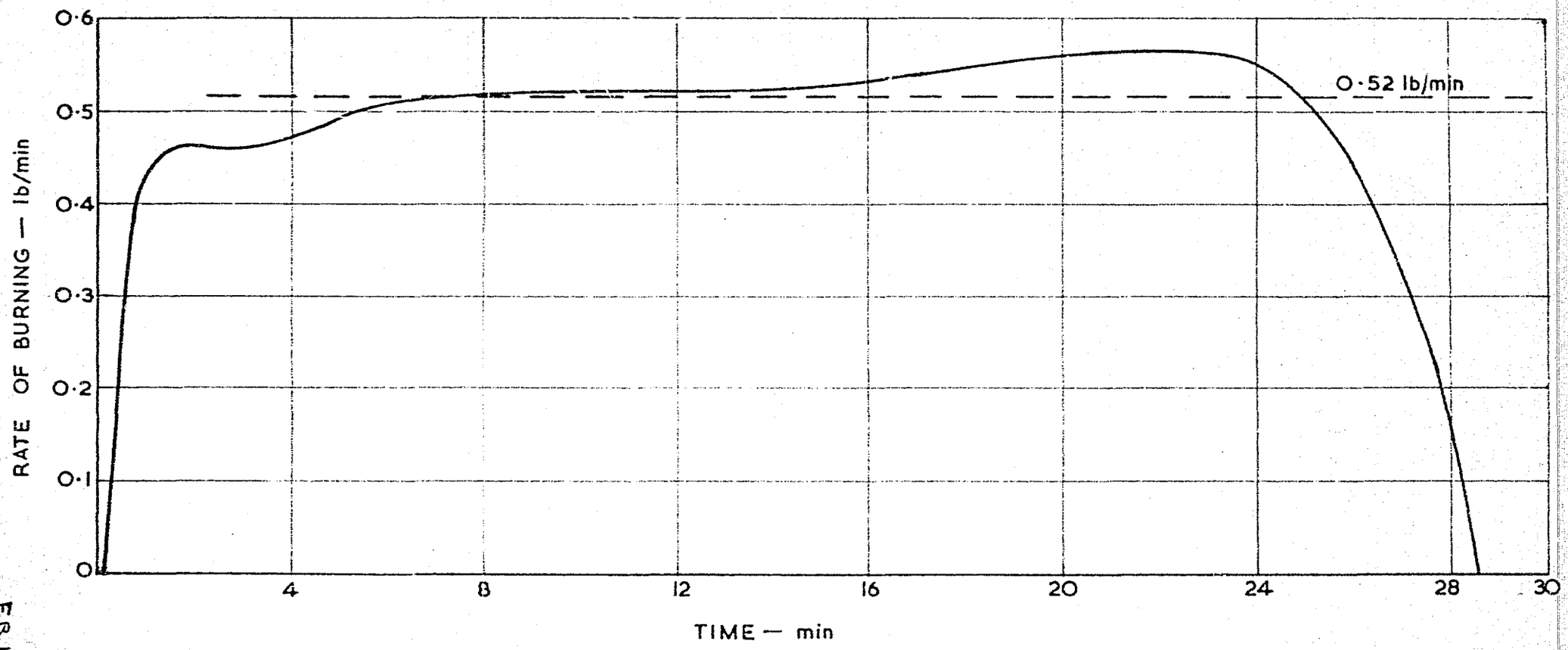

FIG.1. RATE OF BURNING OF METHYLATED SPIRITS IN 17" DIA. TRAY

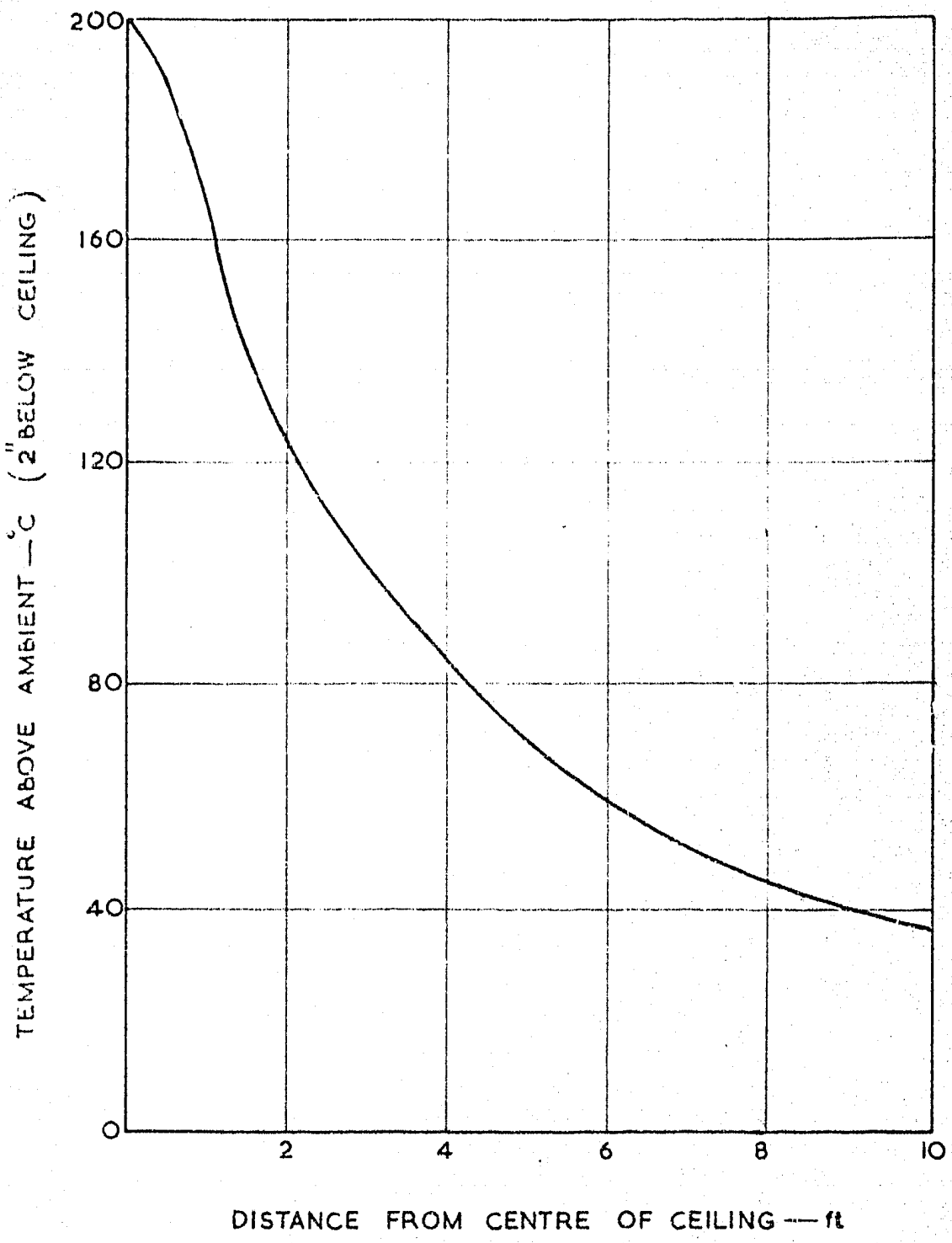

FIG. 2. TEMPERATURE DISTRIBUTION ALONG FLAT CEILING

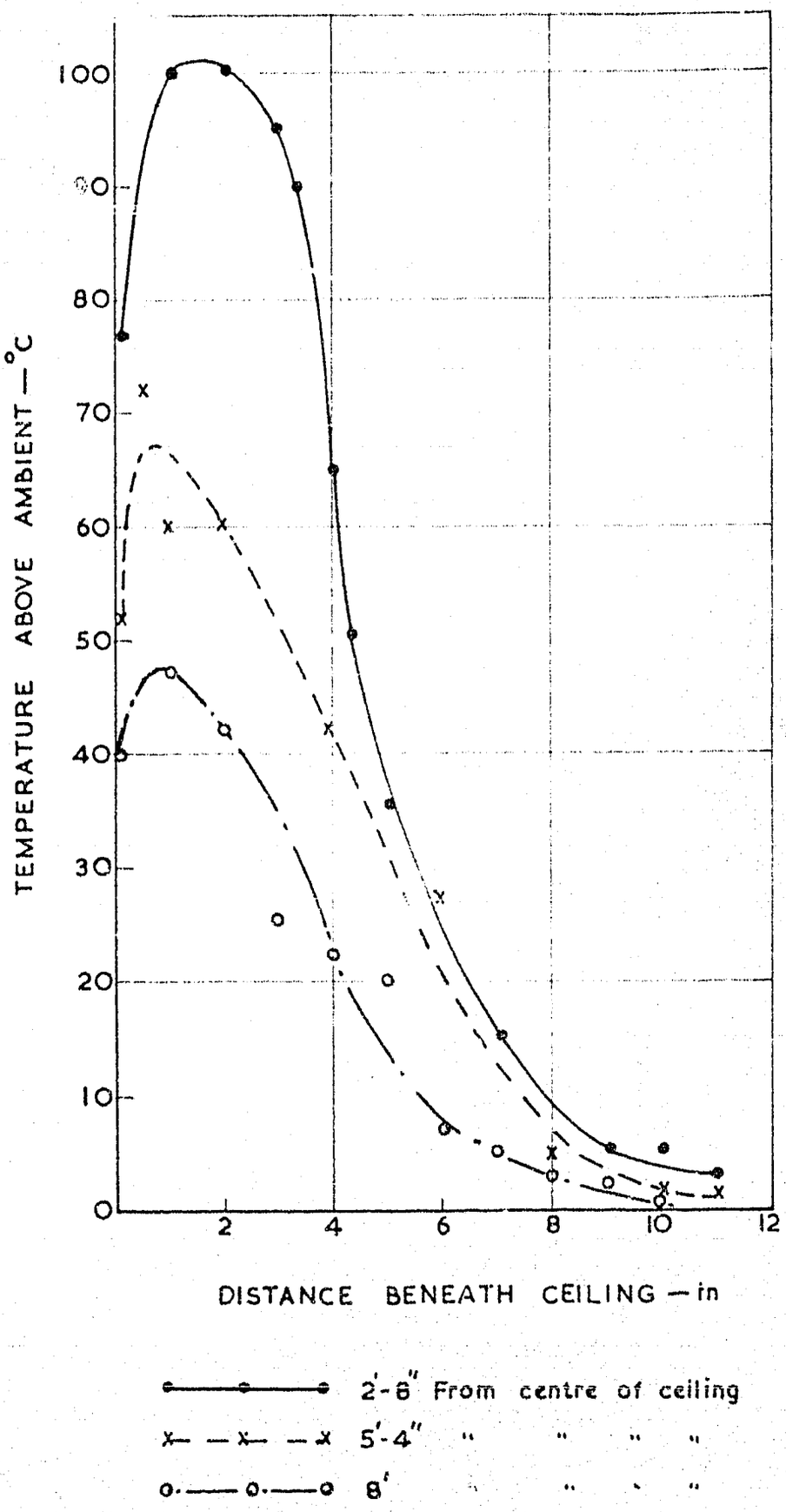

FIG. 3. TEMPERATURE DISTRIBUTION PERPENDICULAR TO CEILING

F.R. 141 1/2026

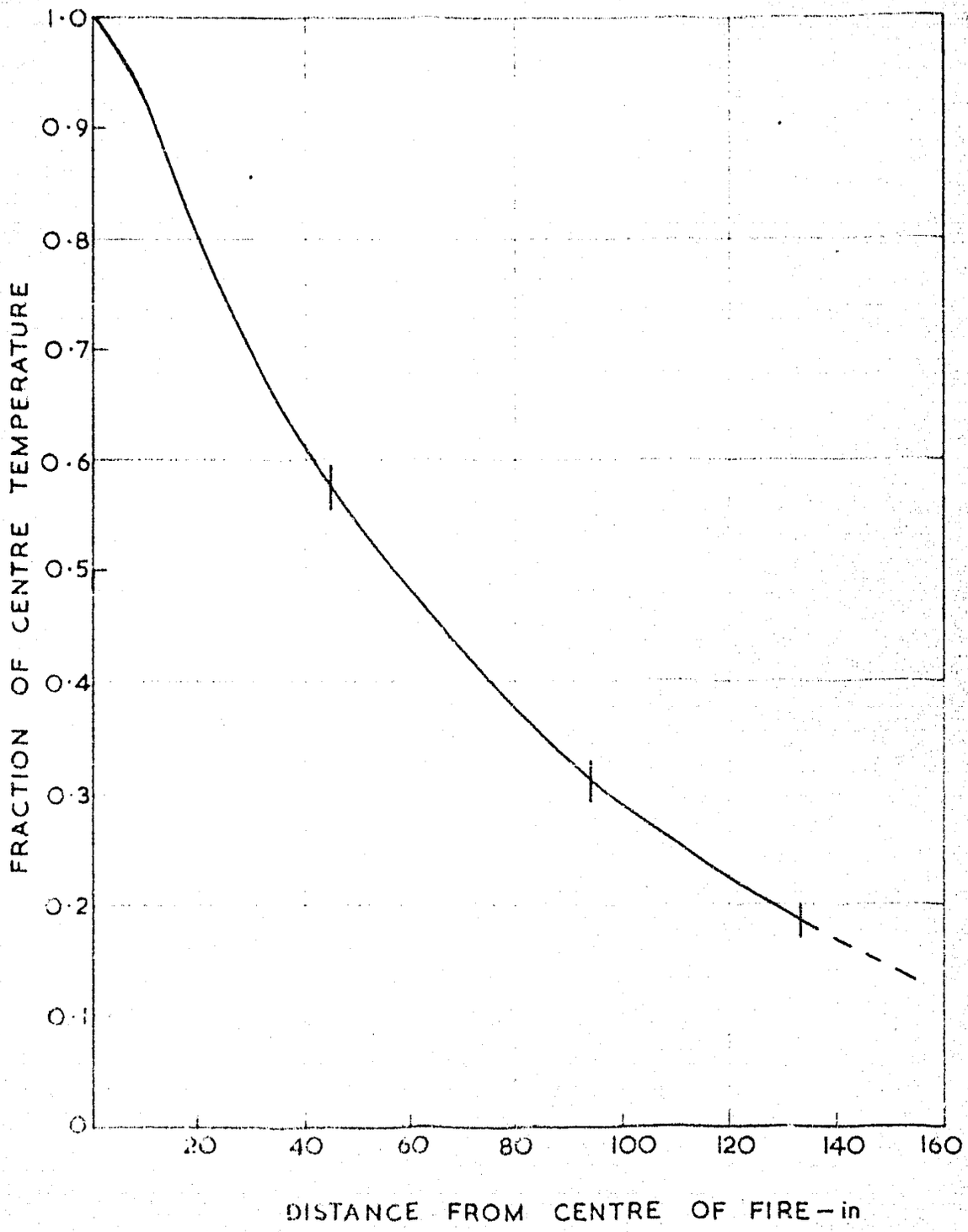

FIG. 6. TEMPERATURE DISTRIBUTION 2" BELOW FLAT CEILING FOR 44 DIA. FIRE

F.R.141 1/2c32.

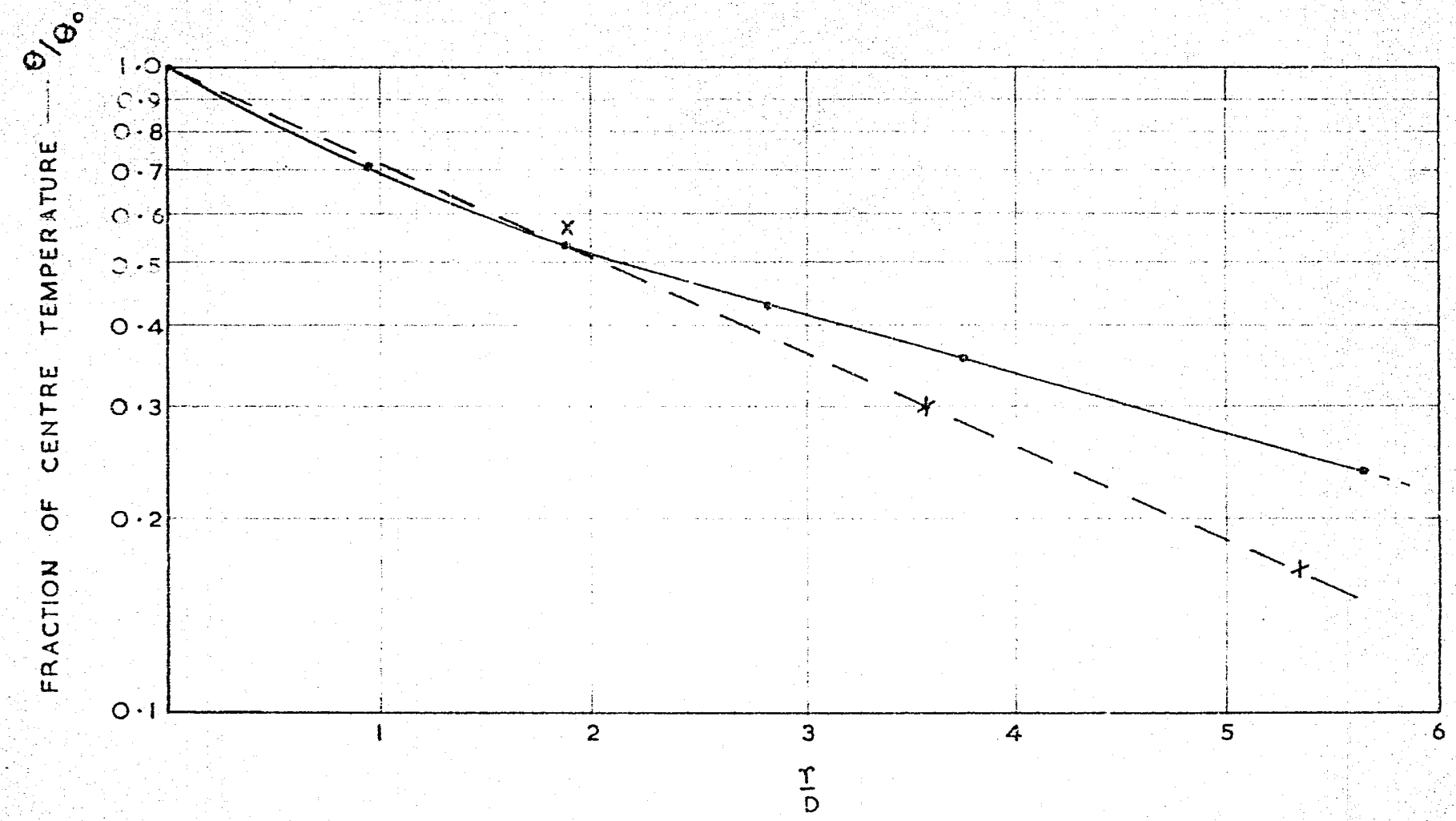

FIG. 7. CORRELATION OF TEMPERATURE DISTRIBUTION FOR TWO FIRES

F.R. 141. 1/2027

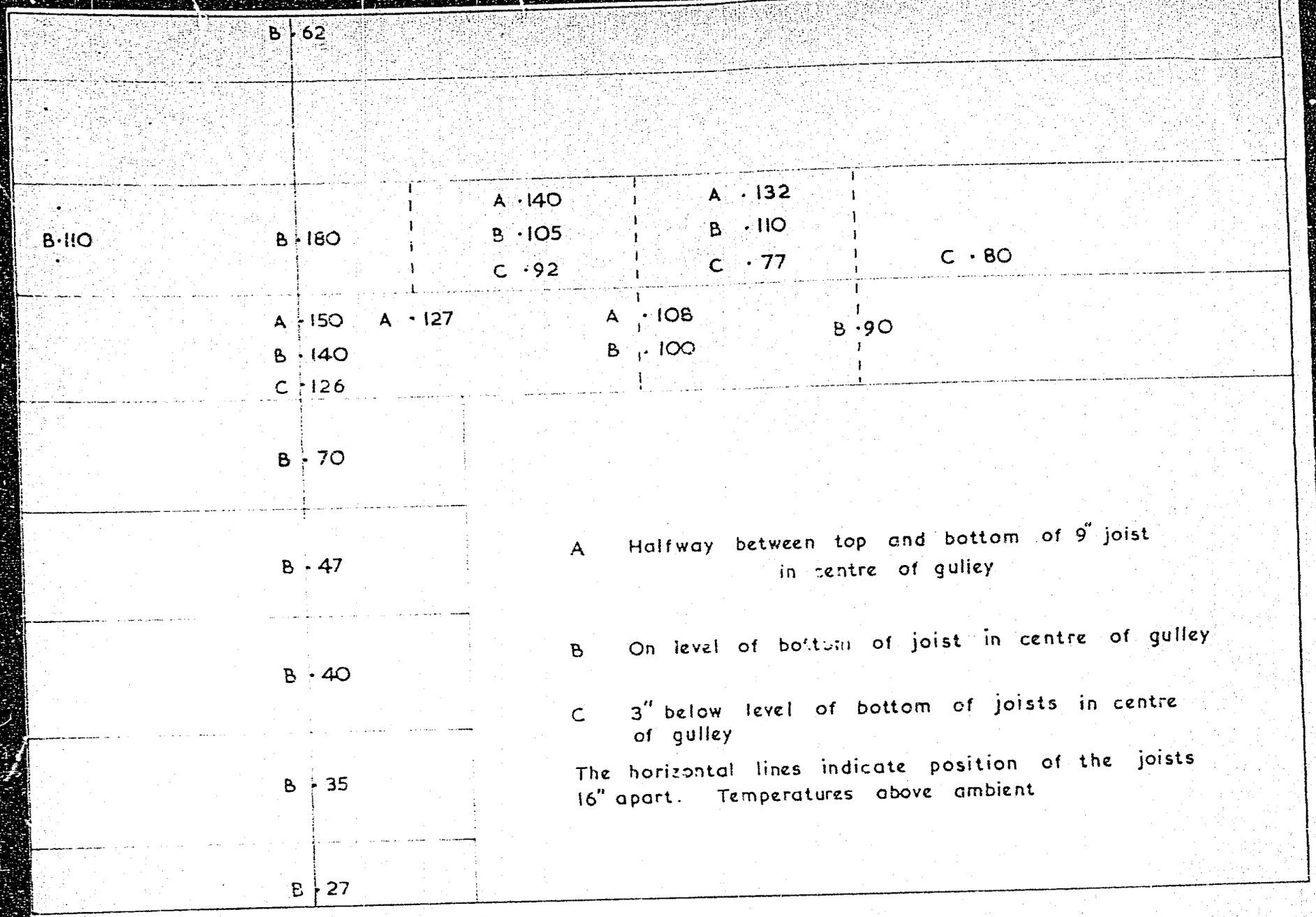

2/191

Fig 9. TEMPERATURE DISTRIBUTION UNDER OPEN-JOISTED CEILING (17in. DIAMETER TRAY)

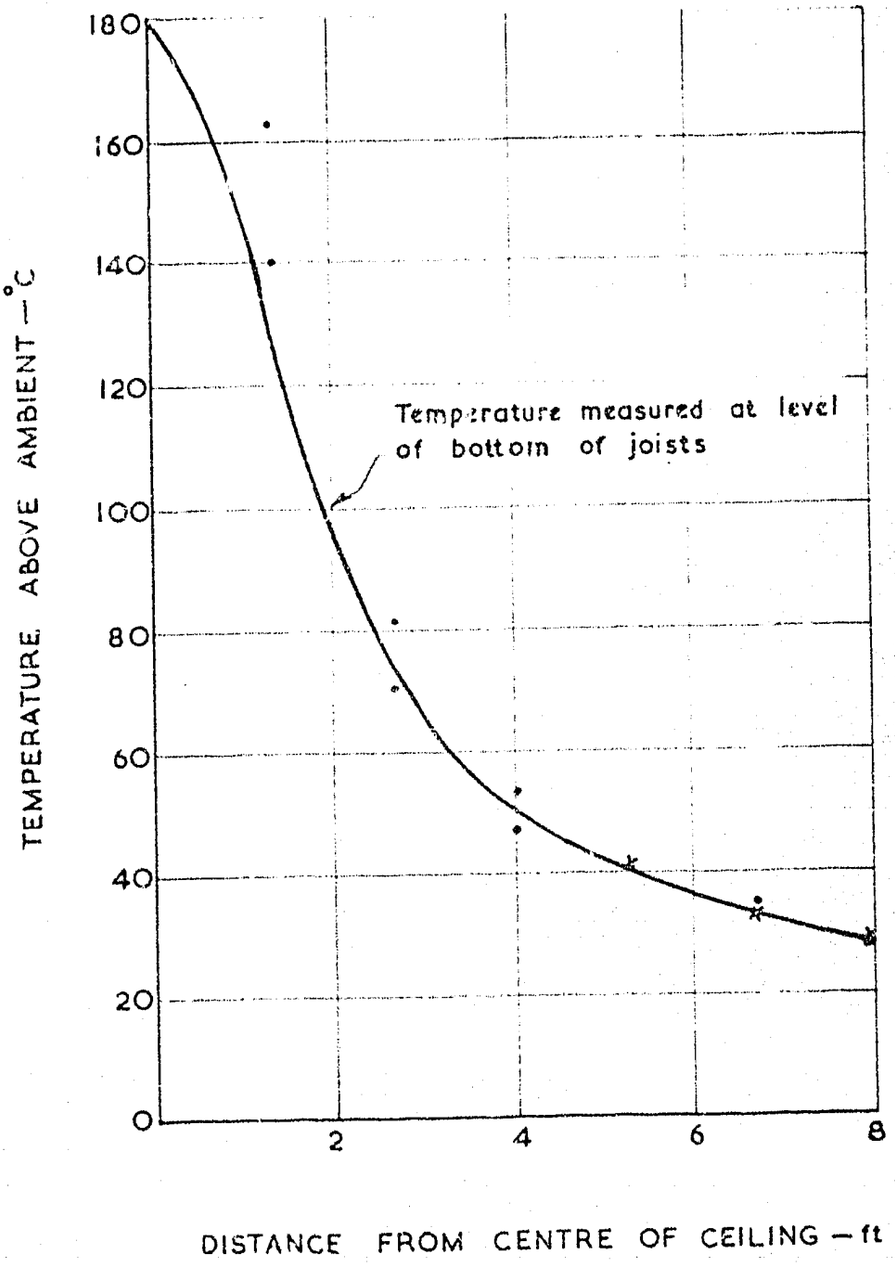

FIG. 10. TEMPERATURE DISTRIBUTION ACROSS JOISTS

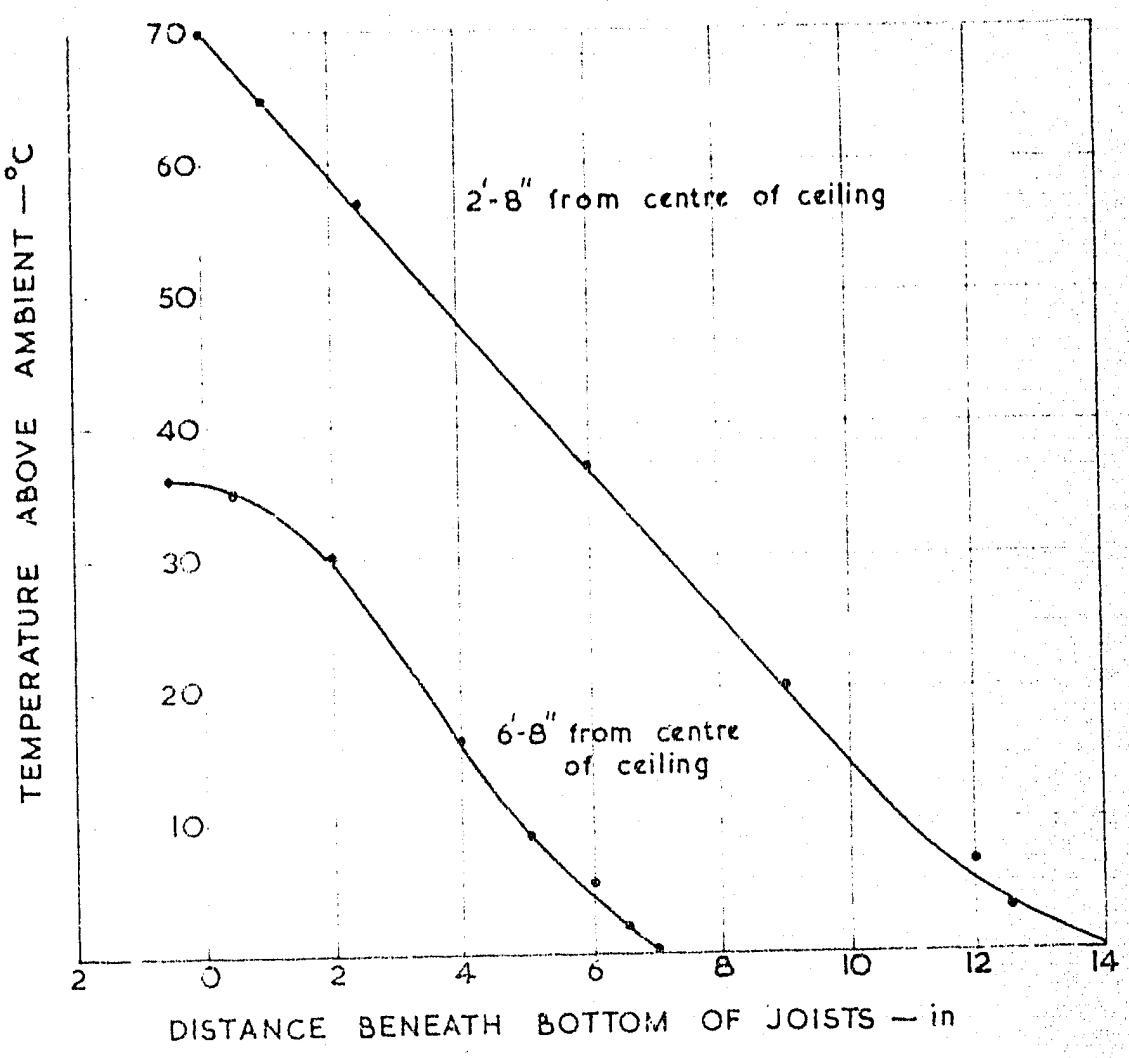

FIG. 11. TEMPERATURE DISTRIBUTION PERPENDICULAR TO JOISTED CEILING

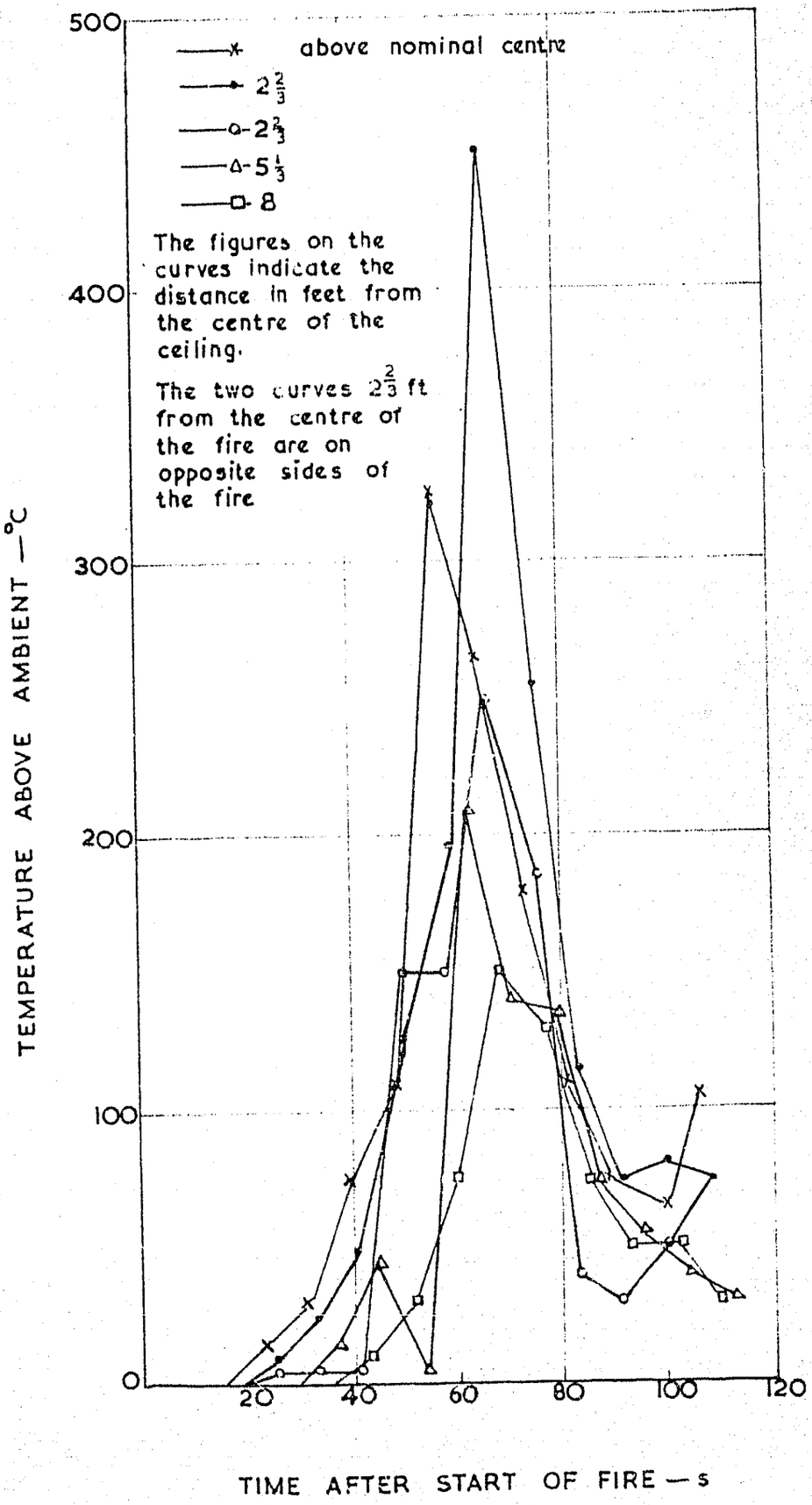

FIG.12. TEMPERATURE DISTRIBUTION ACROSS OPEN JOISTS (THERMOCOUPLES LEVEL WITH BOTTOM OF JOISTS)

F.R.141. 1/2030

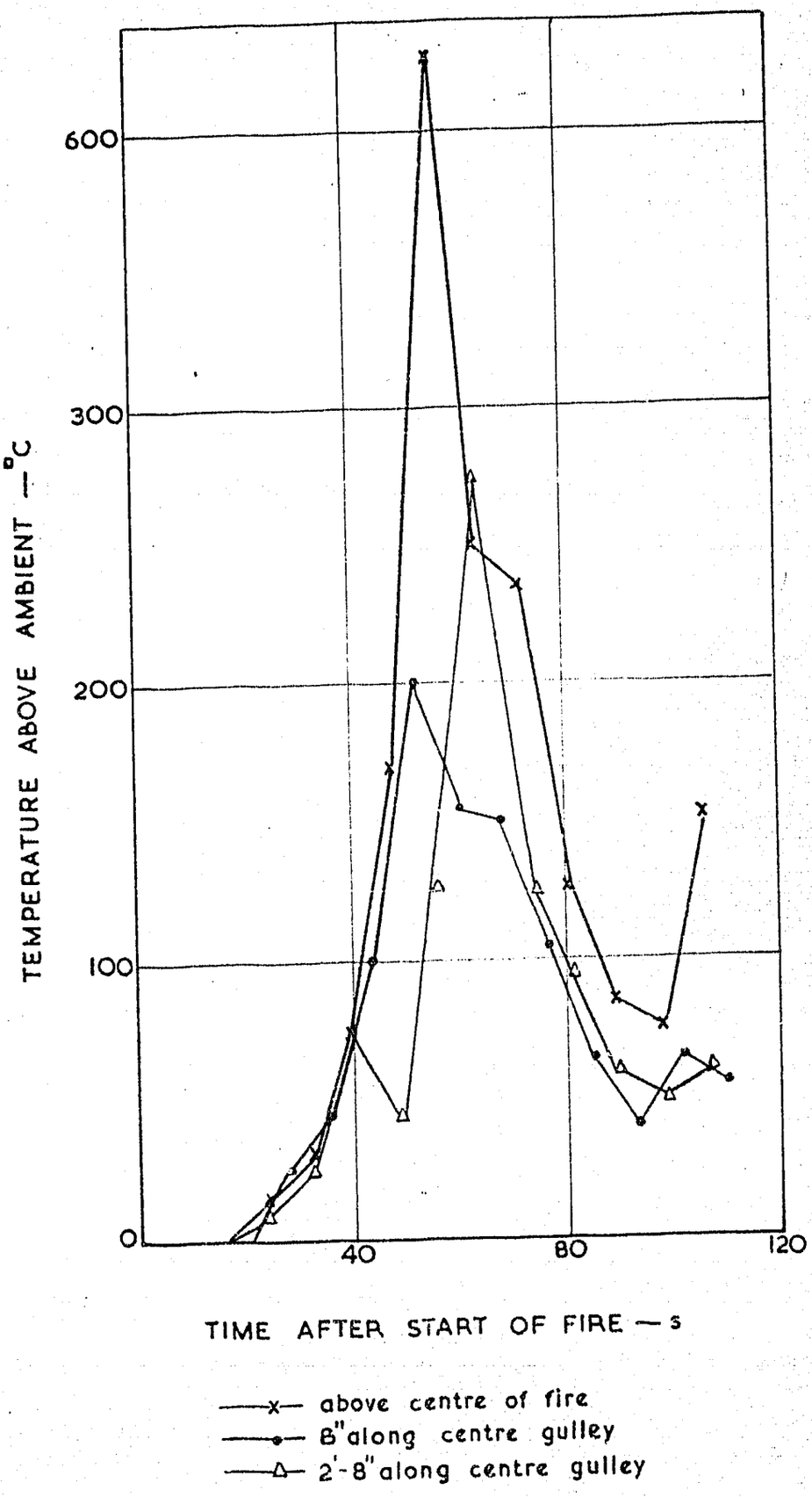

FIG. 13. TEMPERATURE DISTRIBUTION ALONG CENTRE GULLEY

F.R. 141 1/2031